JOURNAL OF CATALYSIS 48, 21–34 (1977)

On the Validity of Kinetic Modeling for Vapor Phase Catalytic Reactions: Isomerization of *n*-Butene to Isobutene[1]

N. S. RAGHAVAN AND L. K. DORAISWAMY

National Chemical Laboratory, Poona, India

Received April 29, 1976; revised February 11, 1977

Experimental kinetic data on the isomerization of *n*-butene to isobutene over fluorinated η-alumina (containing 2.0 wt% F) have been analyzed and a probable Langmuir–Hinshelwood (Hougen–Watson) model in the temperature range 605.5–636.5°K has been proposed based on adsorption of *n*-butene controlling (single site). The values of the equilibrium adsorption constant for isobutene at different temperatures thus obtained (by nonlinear least squares analysis of the kinetic data) have been compared with the corresponding values obtained by adsorption studies under reaction conditions. The values were found to agree to within 12% over the temperature range studied.

NOMENCLATURE

b	Exponent of the dimensionless mass transfer correlation
c	Concentration of the adsorbable gas in the interparticle space [g-mole/cm^3]
F	Feed rate of reactant [g-moles/hr]
G	Mass velocity of reactant [g/hr cm^2]
k_{12}, k_{21}, k_{23}	Rate constants [g-moles/hr g atm]
K_{nB}	Adsorption equilibrium constant for *n*-butene [cm^3/g]
K_{iB}	Adsorption equilibrium constant for isobutene [cm^3/g]
P_g	Bulk gas concentration [atm]
P_s	Surface concentration [atm]
Δp	$P_g - P_s$
r	Reaction rate [g-moles/hr g]
r'	Reaction rate [g/hr cm^2]
Re′	Reynolds number [dimensionless]
t	Time [sec]
t_{0A}	Time of duration of the injection of the adsorbable gas in chromatography [sec]
T	Absolute temperature [°K]
v_i	Linear velocity of the carrier gas in the interparticle space [cm/sec]
W	Weight of the catalyst [g]
X	Fractional conversion
z	Length coordinate of the bed of adsorbent, measured from the inlet side [cm]
α	Interparticle void fraction in the adsorbent bed
β	Intraparticle void fraction [internal porosity] of the adsorbent
δ_0	Expression defined by Eq. (9)
μ_n'	*n*th absolute moment of the chromatographic curve
$[\mu_1']_{\text{inert}}$	First absolute moment for the nonadsorbable gas [sec]
ρ_p	Apparent particle density [g/cm^3]

---

[1] NCL Communication No. 2015.

ISSN 0021-9517

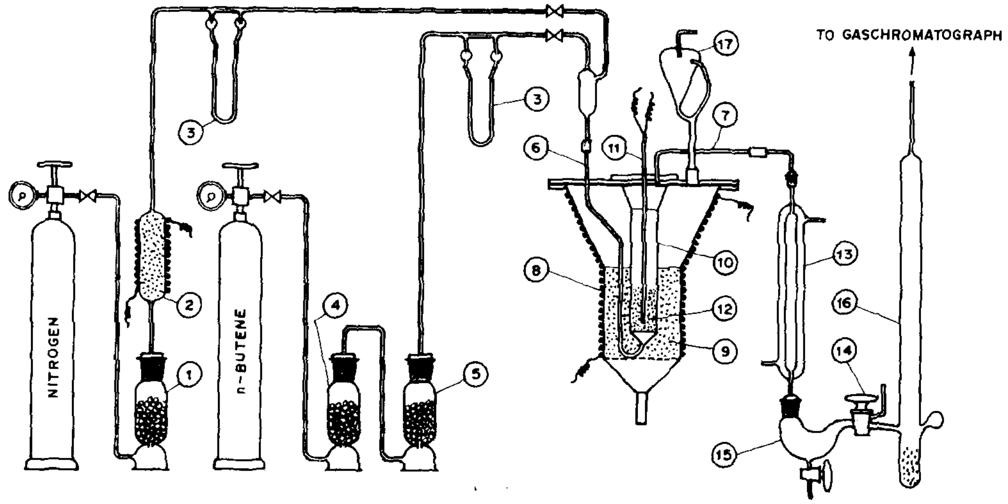

FIG. 1. Experimental assembly. (1) Molecular sieve trap; (2) Tube containing copper bits; (3) Capillary flow meter; (4) Silica gel trap; (5) Fused $CaCl_2$ trap; (6) Feed inlet; (7) Product outlet; (8) Outer heating jacket; (9) Bauxite (fluidized heating bed; (10) Tubular reactor; (11) Thermowell; (12) Granular catalyst; (13) Water condenser; (14) Three-way stop cock; (15) Liquid product collector; (16) Soap bubble flow-meter; (17) Cyclone.

INTRODUCTION

Langmuir's theory of activated adsorption (*1*) and the application of this theory by Hinshelwood (*2*) to a large number of reactions gave rise to the extension of this theory to chemical engineering use by Hougen and Watson (*3*). This was followed by derivation of generalized rate equations for many types of reactions by Yang and Hougen (*4*). Since then many sophisticated methods have been suggested for choosing among rival models and for obtaining precise parameter estimates and these have been widely reviewed [see, for example, Bard and Lapidus (*5*), Kittrell (*6*) and Reilly and Blau (*7*)].

Kinetic studies of reactions catalyzed by solids based only upon overall reaction rates are usually not sensitive enough to establish a reliable model, or to permit discrimination among different plausible models as pointed out by Mezaki (*8*). Supplementary experiments to obtain the adsorption equilibrium constants of the individual components and a comparison of these values with those obtained from the proposed model by statistical techniques will enhance the validity of the rate equation.

Kabel and Johnson (*9*) compared the adsorption equilibrium constants obtained from the proposed Langmuir–Hinshelwood model for the reaction, vapor phase dehydration of ethanol to diethyl ether in the presence of cation exchange resin as catalyst, with those obtained from a static adsorption system. However, the static adsorption method is likely to lead to decomposition of the components due to prolonged contact with the catalyst, and it is therefore desirable to measure the adsorption parameters at reaction temperatures by an independent method wherein the contact time between the components and the solid catalyst is very small.

No experimental data are yet available which might form a basis for an objective assessment of the statistical methods of model discrimination and selection. The present work was therefore undertaken to fill this gap using the model reaction—isomerization of *n*-butene to isobutene on a η-alumina catalyst, for the purpose. In summary, it was sought to determine the adsorption equilibrium constants for *n*-butene and isobutene from the statistical methods of kinetic modeling and to compare these values with those obtained from chromatographic methods under reaction conditions (*10*) without resort to kinetic modeling. Agreement between these two sets of values would impart greater reliability to the kinetic method of modeling.

PARAMETER VALUES FROM KINETIC MODELING

Experimental Methods

n-Butene [99.5% purity] prepared by the catalytic dehydration of *n*-butanol over basic alumina was used as the starting material for the isomerization reaction leading to the formation of isobutene.

Fluorinated η-alumina containing 2 wt% F was prepared by impregnating η-alumina [activated at 600°C] with ammonium fluoride from a solution containing the appropriate quantity of fluorine, drying at 120°C for 16 hr, and activating at 400°C in the presence of air.

The apparatus used in the kinetics experiments is shown schematically in Fig. 1. The reactor used for carrying out the kinetic runs was an integral reactor of 0.75 in. i.d. and 14 in. height, provided with a thermocouple well which extended from the top of the reactor to just above the wire mesh support for the catalyst.

The other units of the reactor assembly were: capillary flowmeters to measure gas flow rates, a water condenser to condense liquid products, a soap bubble flowmeter to measure the outlet flow of the gas, and a NCL designed gas chromatographic unit which was connected in series with the reactor assembly to facilitate on-stream analysis of the outlet gas from the reactor.

The temperature of the catalyst bed was maintained at the required constant level by careful control of the rate of fluidizing air and power input. A Chromel–alumel thermocouple was used for the temperature measurement. The thermocouple was calibrated against a standard thermometer which had a least count of 0.5°C. A portable potentiometer (with a least count of 0.01 mV) was used for the measurement of the thermocouple potential.

The reactor was packed with -40 to $+60$ B.S. mesh freshly activated catalyst to a bed depth of about 15 cm and the heating was begun while a continuous flow of nitrogen through the bed was maintained. After attaining the required temperature, nitrogen flow was stopped and *n*-butene flow was started. The kinetic runs were conducted after the attainment of steady state with regard to temperature, flow rate of reactant gas and outlet concentration.

The reaction product was analyzed with a gas chromatograph provided with a thermal conductivity detector at room temperature with a 12 ft long column of silver nitrate–ethylene glycol stationary phase supported on Chromosorb-W-Regular. Hydrogen gas free from moisture was used as carrier gas at a flow rate of 50 cm^3/min. A 6-port gas sampling valve which allowed the venting of product gas when not to be sampled was used for injecting a fixed quantity [0.5 cm^3 in this case] of the outlet gas into the column. Determination of the percentage of isobutene was achieved by knowing the ratio of the area of the isobutene peak after product separation and pure isobutene, along with a knowledge of inlet and outlet rates of flow of *n*-butene. A run consisted of product analysis at each of a series of flow rates with other conditions remaining unaltered.

In the organization of the experimental program for determining the rate parameters, the following ranges of main variables were covered: temperature, 605.5–636.5°K; reciprocal space velocity, 50–650 g hr/g mole.

TABLE 1

Experimental Kinetic Data[a]

Run No.	W/F	X_{iB} $\times 10^2$	P_{nB}	P_{iB}	r(exptl) $\times 10^3$	r(calcd) $\times 10^3$
1	2	3	4	5	6	7
Temperature: 605.5°K						
A_1	194.0	2.90	0.9070	0.0271	0.1492	0.1431
A_2	307.5	4.20	0.8950	0.0392	0.1361	0.1317
A_3	450.0	5.50	0.8830	0.0514	0.1220	0.1267
A_4	525.0	6.60	0.8725	0.0616	0.1196	0.1139
A_5	601.0	6.92	0.8690	0.0646	0.1152	0.1119
A_6	232.0	2.45	0.6830	0.0172	0.1050	0.1141
A_7	355.0	3.68	0.6740	0.0257	0.1033	0.1065
A_8	503.0	5.10	0.6650	0.0357	0.1011	0.0992
A_9	625.5	5.83	0.6590	0.0408	0.0930	0.0954
A_{10}	208.0	1.50	0.4602	0.0070	0.0838	0.0809
A_{11}	300.0	2.08	0.4575	0.0097	0.0821	0.0789
A_{12}	462.0	2.81	0.4541	0.0131	0.0787	0.0765
A_{13}	540.0	3.19	0.4523	0.0149	0.0716	0.0754
A_{14}	660.0	3.56	0.4506	0.0166	0.0707	0.0743
Temperature: 621.0°K						
B_1	120.0	5.2	0.8816	0.0483	0.4321	0.4356
B_2	279.0	9.25	0.8478	0.0864	0.3310	0.3129
B_3	440.0	12.50	0.8174	0.1167	0.2838	0.2729
B_4	544.0	13.20	0.8115	0.1227	0.2432	0.2471
B_5	639.4	15.25	0.7917	0.1424	0.2387	0.2434
B_6	117.0	3.75	0.6744	0.0263	0.3207	0.3081
B_7	211.7	6.30	0.6565	0.0441	0.2974	0.2793
B_8	347.6	9.10	0.6369	0.0637	0.2615	0.2512
B_9	478.0	10.75	0.6253	0.0753	0.2243	0.2361
B_{10}	586.0	12.45	0.6134	0.0872	0.2121	0.2217
B_{11}	129.0	2.63	0.4549	0.0123	0.1401	0.1460
B_{12}	172.0	3.31	0.4518	0.0154	0.1378	0.1429
B_{13}	266.0	4.58	0.4458	0.0214	0.1349	0.1372
B_{14}	400.0	5.97	0.4393	0.0279	0.1330	0.1317
B_{15}	524.0	6.45	0.4371	0.0301	0.1304	0.1293
B_{16}	656.0	7.84	0.4306	0.0366	0.1277	0.1238
Temperature: 636.5°K						
C_1	92.0	9.00	0.8501	0 0841	0.9775	1.0090
C_2	180.0	15.50	0.7894	0.1448	0.8604	0.8395
C_3	301.0	21.50	0.7333	0.2008	0.7121	0.7014
C_4	390.0	23.70	0.7128	0.2214	0.5925	0.6032
C_5	469.3	27.00	0.6819	0.2522	0.5749	0.5879
C_6	57.0	4.70	0.6677	0.0329	0.8241	0.8636
C_7	144.8	10.30	0.6285	0.0722	0.7109	0.7511
C_8	239.4	16.30	0.5864	0.1142	0.6806	0.6415
C_9	380.7	20.80	0.5549	0.1457	0.5457	0.5658
C_{10}	80.0	4.06	0.4483	0.0189	0.2548	0.2489
C_{11}	152.0	1.52	0.4368	0.0304	0.2467	0.2360
C_{12}	266.0	9.84	0.4213	0.0459	0.2282	0.2192
C_{13}	338.0	11.40	0.4140	0.0532	0.2101	0.2115
C_{14}	488.0	13.43	0.4045	0.0627	0.2043	0.2016

[a] Runs A_1–A_5, B_1–B_5, and C_1–C_5 were conducted with pure *n*-butene. Runs A_6–A_9, B_6–B_{10}, and C_6–C_9 were conducted with 75 vol% *n*-Butene and 25 vol% nitrogen. Runs A_{10}–A_{14}, B_{11}–B_{16}, and C_{10}–C_{14} were conducted with 50 vol% *n*-Butene and 50 vol% nitrogen.

Results

Complete integral conversion results of the reaction rate studies are shown in Table 1. They include studies at three temperature levels, 605.5, 621.0, and 636.5°K. Feed compositions include pure *n*-butene feeds and *n*-butene–nitrogen mixtures.

Plots of the experimental data are shown in graphical form in Figs. 2, 3, and 4, which illustrate the effect of temperature and space velocity upon conversion for three initial compositions.

The rate of reaction was calculated by numerical differentiation of the data using Newton's method from the relation,

$$r = \frac{dX}{d[W/F]}, \tag{1}$$

where r is the reaction rate, X the fractional conversion, and W/F the reciprocal space velocity.

Mass Transfer Considerations

In this work the resistance due to pore diffusion was overcome by using small size catalyst particles (−40 to +60 B.S. mesh). The rate data were also analyzed by the method of Weisz and Prater (*11*). The results showed that the rate data were free from the influence of pore diffusional resistance.

The mass transfer effect due to gas film resistance was evaluated by the method of Ford and Perlmutter (*12*) who derived the expression,

$$\frac{\Delta p}{p_g} = \frac{d \ln r'/d \ln G}{b}, \tag{2}$$

by equating the rates of mass transfer and chemical reaction under conditions of steady state. In the case of gas–solid reactions, b in the above equation equals 0.59 for $\mathrm{Re}' > 350$ (*13*) and 0.49 for $\mathrm{Re}' < 350$ (*14*). In the present case, since Re' was found to be always less than 350, Eq. (2) becomes,

$$\frac{\Delta p}{p_g} = \frac{d \ln r'/d \ln G}{0.49}. \tag{3}$$

Plots of ln r' vs ln G (where G is the total mass flow rate) were drawn for different values of reciprocal space velocity and it was found that the slope $d \ln r'/d \ln G$ and hence the ratio $\Delta p/p_g$ approached zero asymptotically as the mass flow rate was increased. Therefore, in order to ensure the absence of external mass transfer resistance, flow rates were so chosen for each value of the reciprocal space velocity that $\Delta p/p_g$ was less than 0.05.

Reaction modeling

The reaction of *n*-butene over fluorinated η-alumina containing 2 wt% F can be represented as

$$\begin{array}{ccc} A & \underset{k_{21}}{\overset{k_{12}}{\rightleftharpoons}} & B \\ [1] & & [2] \end{array}$$

where A, B (as well as 1, 2) represent *n*-butene and isobutene, respectively. Choudhary and Doraiswamy (*15*), however, also observed the formation of polyisobutene and represented the reaction as

$$\begin{array}{ccccc} A & \underset{k_{21}}{\overset{k_{12}}{\rightleftharpoons}} & B & \xrightarrow{k_{23}} & P\ , \\ [1] & & [2] & & [3] \end{array}$$

where P (as well as 3) represents polyisobutene.

The thermodynamic equilibrium constant K of the reversible step was calculated at all the temperatures involved from the reported thermochemical data [Choudhary (*16*)].

Eleven different Hougen–Watson models and the simple power law model: $r = k \times (p_{nB} - p_{iB}/K)$ were considered for selecting the most suitable one for the isomerization reaction. The power law model gave very large deviations (28%) between the observed and calculated rates and was therefore rejected. In the case of Hougen–Watson models, the values of the parameters to be used as initial guesses while carrying our nonlinear least squares analysis of the data were obtained from the linear least squares analysis. The statistical

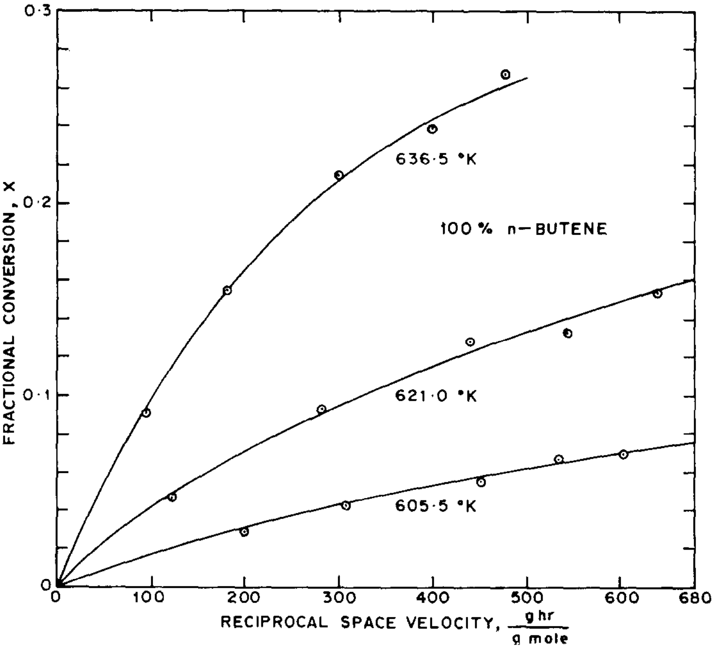

FIG. 2. Conversion vs reciprocal space velocity plots for the isomerization of *n*-butene.

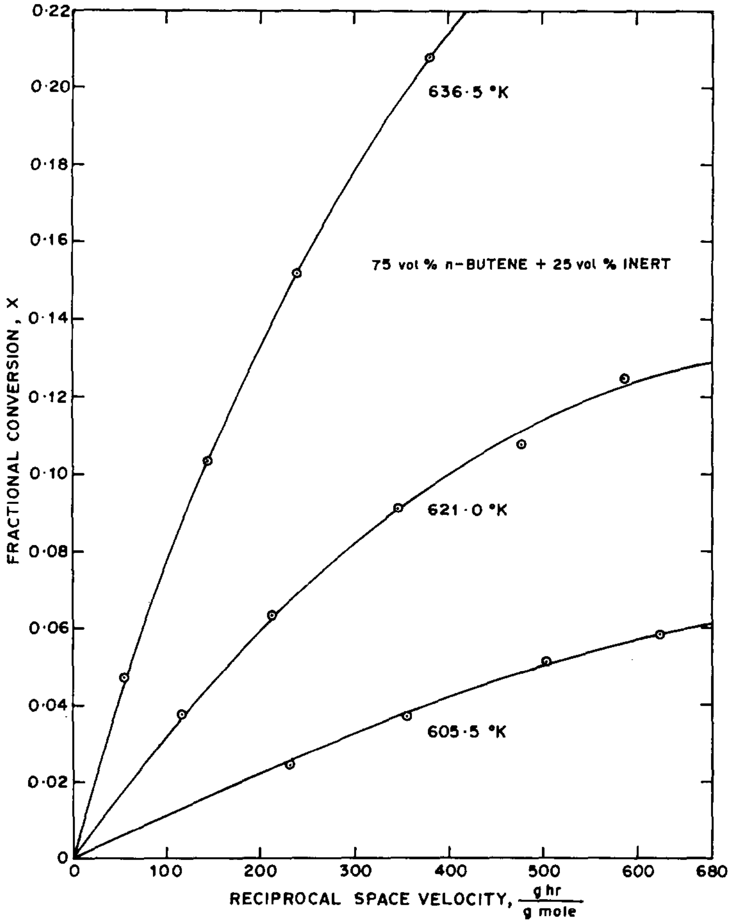

FIG. 3. Conversion vs reciprocal space velocity plots for the isomerization of *n*-butene.

analysis of the model parameters for their significance and fit was performed at 95% confidence level.

When the models were subjected to nonlinear least squares analysis, it was found that 10 out of the 11 models considered yielded negative values of the adsorption equilibrium constant which were significantly different from zero. The only model which gave positive values at all the temperatures studied was based on the single site mechanism (adsorption of *n*-butene controlling). The *F* test also confirmed the adequacy of this of the model over the entire temperature range studied, as the calculated values of *F* were found to be less than the table values.

The selected model could be represented as

$$r = \frac{k[p_{n\mathrm{B}} - p_{i\mathrm{B}}/K]}{1 + K_{i\mathrm{B}}p_{i\mathrm{B}}}. \tag{4}$$

The validity of the model was further confirmed by comparing the estimated rates with the observed rates at the three temperatures studied, as shown in Fig. 5.

The adsorption equilibrium constants for isobutene obtained from the proposed model for all the three temperatures are given in Table 2 in units of cm^3/g catalyst.

PARAMETER VALUES FROM ADSORPTION MEASUREMENT UNDER REACTION CONDITIONS

The objectives of the adsorption studies are to determine the adsorption equilibrium constants for isobutene and *n*-butene at the reaction temperatures and to compare the values obtained with those extracted from the proposed Hougen–Watson model.

Tamaru (*17*, *18*) was among the first to initiate adsorption measurements during surface catalysis with simultaneous measurement of reaction rate. Tamaru (*19*) and Nakanishi and Tamaru (*20*) also suggested the gas chromatographic method for the determination of adsorption and subsequently the surface area of the catalyst during catalysis. Eberly (*21*) carried out high temperature adsorption studies of hydrocarbons on 13 x molecular sieve, alumina and other porous solids by a pulse flow technique using gas chromatography. He could calculate the heat of adsorption and adsorption equilibrium constant for benzene on η-alumina by this method. Eberly (*22*) also developed a method involving a continuous flow of adsorbate through a column of initially unsaturated adsorbent by means of an inert nonadsorbable carrier gas. After saturation, the adsorbed material was eluted by the pure carrier gas alone. From an analysis of the composition of the effluent stream as a function of time, he could calculate the adsorption isotherm for *n*-butene on silica gel.

Schneider and Smith (*10*) developed a method based on the theory proposed by Kubin (*23*, *24*) and Kucera (*25*) for relating the moments of the effluent concentration wave from a bed of adsorbent

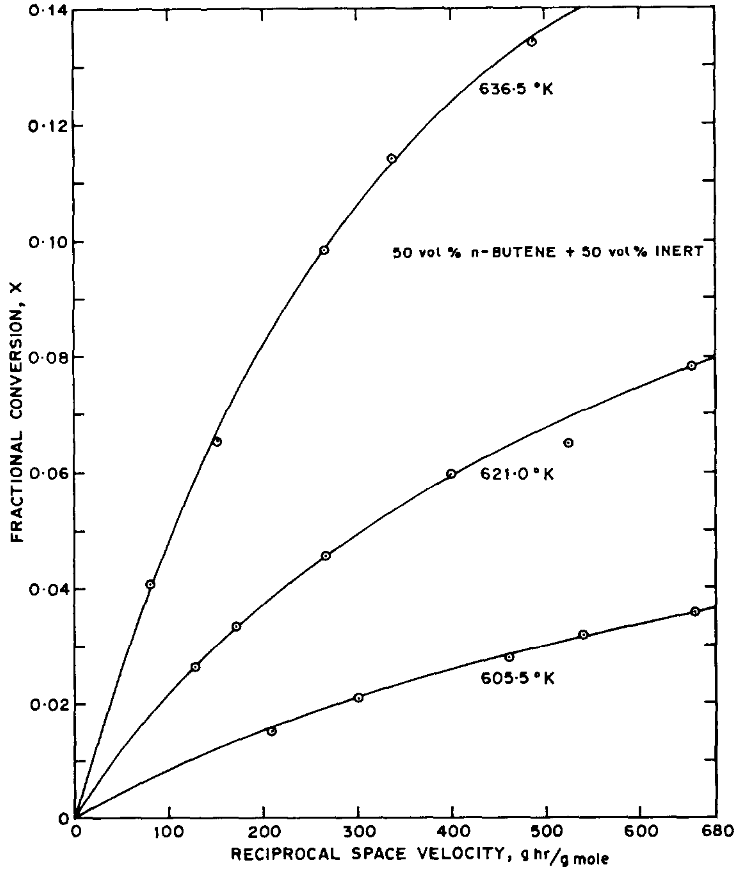

FIG. 4. Conversion vs reciprocal space velocity plots for the isomerization of *n*-butene.

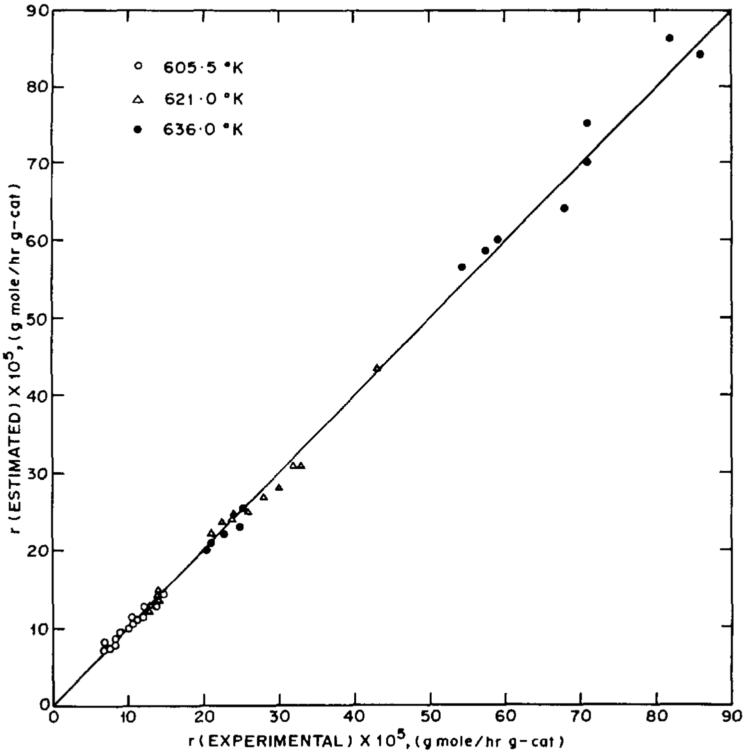

FIG. 5. Comparison of experimental rates with those estimated from the proposed model.

particles to the rate constants associated with the various steps in the overall adsorption process and used this method for determining the adsorption equilibrium constants, rate constants and intraparticle diffusivities for various hydrocarbons on silica gel.

The theory proposed by Kubin [*23*, *24*] and Kucera (*25*) greatly contributed to the improvement of the theoretical treatment of gas–solid chromatography. Kubin (24) solved a set of differential equations which described the movement of an adsorbable substance in a chromatographic column and obtained explicit expressions for the moments of the chromatographic curves, $c[z, t]$. He described the pulse input by a square function (*23*, *24*),

$$\begin{aligned} c &= c_0 \quad \text{at} \quad z = 0 \quad \text{for} \quad 0 \le t \le t_{0A}, \\ c &= 0 \quad \text{at} \quad z = 0 \quad \text{for} \quad t > t_{0A}, \end{aligned} \tag{5}$$

where t_{0A} is the injection time of the adsorbate gas of concentration c_0.

The nth absolute moment μ_n' of the function $c[z, t]$ is defined as

$$\mu_n' = m_n/m_0, \tag{6}$$

where

$$m_n = \int_0^\infty t^n c[z, t]dt[n = 0, 1, 2, 3, \ldots]. \tag{7}$$

The first absolute moment μ_1' characterizes the position of center of gravity of the chromatographic curve, which can be evaluated from the experimental chromatographic curves of the effluent from the column by using Eqs. (6) and (7). Data at different carrier gas velocities will give the moment as a function of velocity.

Schneider and Smith (*10*) correlated the first absolute moment with the bed length of the solid particles, interstitial carrier gas velocity, external porosity, internal void fraction, particle density, injection time of the adsorbable gas and the adsorption equilibrium constant by means of the following equations:

$$\mu_1' = \left[\frac{z}{v_i}\right][1 + \delta_0] + [t_0A/2], \qquad (8)$$

where

$$\delta_0 = [(1 - \alpha)\beta/\alpha][1 + (\rho_p/\beta)K_A]. \qquad (9)$$

In the present work, the method proposed by Schneider and Smith (*10*) was followed to obtain the first absolute moment of the chromatographic peaks and hence the adsorption equilibrium constants.

Experimental Methods

Chromatographic curves of isobutene and *n*-butene on η-alumina [containing 2% wt F] at temperatures ranging from 574.5 to 636.5°K for isobutene and 559 to 590°K for *n*-butene and at atmospheric pressure were measured. Nitrogen was used as the carrier gas and the concentrations of isobutene and *n*-butene were chosen after a study of the effect of their concentration on the first absolute moment at three different temperatures of study. The η-alumina particles used were of -40 to $+60$ B.S. mesh size [0.34 mm] and the interstitial velocity of carrier gas ranged from 8 to 35 cm/sec. By a separate experiment it was found that at the minimum velocity for each set of runs and at the concentration of isobutene and *n*-butene chosen for this study, the conversion of isobutene and *n*-butene to each other at all the temperatures was too small to measure even by gas chromatography.

Adsorbent

The alumina used for this study was taken from the same batch of catalyst used for the kinetic runs. Before each run, the adsorbent was conditioned in the apparatus for 15 hr at the highest temperature of study with a continuous flow of dry nitrogen. The physical properties of the alumina catalyst were, BET surface area, 141 m^2/g; pore volume, 0.322 cm^3/g; internal void fraction $\beta = 0.485$, particle density $\rho_p = 1.41$ g/cm^3. The average pore radius was 42 Å.

TABLE 2

Adsorption Coefficients on η-Alumina Catalyst from Kinetics and Chromatographic Measurements

Temp T [°K]	K_{iB} (cm^3/g)		K_{nB} (cm^3/g)	
	From kinetic measurements	From adsorption studies	From kinetic measurements	From adsorption studies
636.5	1.30	1.64	≈0	0
621.0	3.69	4.30	≈0	0
605.5	6.58	6.65	≈0	0
590.0	—	11.77	—	1.15
574.5	—	24.96	—	1.43
559.0	—	—	—	1.84

Gases

The "ultrahigh pure" grade nitrogen was dried by passing through a trap containing 5A molecular sieve and then passed through a tube containing copper bits heated to 300°C in order to remove trace amount of oxygen. *n*-Butene [99.5% purity prepared by the catalytic dehydration of *n*-butanol over basic alumina and isobutene prepared by dehydration of tertiary butyl alcohol over cation exchange resin were dried before use by passing through traps containing silica gel and fused calcium chloride. Mixtures of hydrocarbon and nitrogen of known volumes were obtained by adjusting the flow rates of the individual gases in capillary flow meters.

Parameter [Adsorption Constant] Estimation from Chromatographic Measurements

The gas chromatographic unit used was a NCL designed one with flame ionization detector. Instead of the inbuilt oven, a separate fluidized bed heating bath was

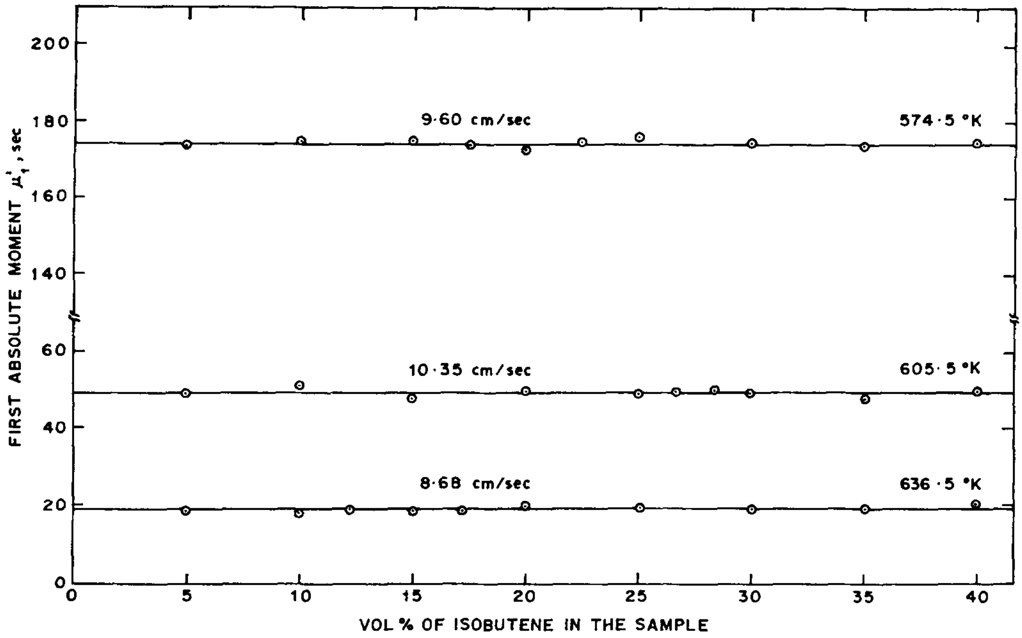

FIG. 6. Effect of isobutene concentration on the first absolute moment.

used in order to achieve gradientless conditions in the column containing the catalyst particles [which was essentially a U-tube connected to the top flange of the heating bath]. A 0.125 in. o.d. stainless steel capillary tubing was used for connecting the U-tube to the carrier gas inlet and to the flame ionization detector and thereby the dead volume in the system was made negligible. A six port sampling valve built in the chromatograph permitted injection of a square wave in concentration. The experimental assembly was similar to the one used for the kinetic study and shown in Fig. 1 except for the presence of the U-tube in the fluidized bed heating bath in place of the integral reactor, and the stainless steel capillary tubing connecting the U-tube to the gas inlet and the flame ionization detector.

A fixed quantity (0.5 ml in this case) of hydrocarbon–nitrogen mixture was injected into the U-tube through the gas sampling valve whenever the chromatographic curves were to be measured.

The U-tube (containing the catalyst particles) was made of stainless steel tubing of 0.25 in o.d. and 27.8 cm length. The external porosity α for the packing in the U-tube was found to be 0.38.

It is known that in the case of nonlinear isotherms, the moments of the chromatographic curves will depend on the concentration of the injected pulse. Hence, in order to be sure that the data collected in this work were pertaining to the linear region of the adsorption isotherm, a few injections of varying concentrations of isobutene were made at a fixed carrier gas velocity and at three temperatures of operation. The results are plotted in Fig. 6. It could be seen that up to a concentration of 40 vol% of hydrocarbon in the sample there was no change in the first absolute moment. Hence, a concentration of 25 vol% of hydrocarbon was chosen for all the runs to evaluate the first absolute moment of the chromatographic curves in this study.

Calculation of First-Absolute Moment and Hence the Adsorption Equilibrium Constants

The first absolute moment of the chromatographic curves were evaluated numerically with the help of a IBM 1620 digital computer using Simpson's rule. In place of concentration in Eq. (7), the deflection of the recorder connected with the flame ionization detector at the column outlet was used. Eqs. (8) and (9) lead to

$$\frac{[\Delta\mu_1' - (t_{0A}/2)]}{[(1-\alpha)/\alpha]\beta} = \frac{\rho_p K_A}{\beta}[z/v_i], \qquad (10)$$

where

$$\Delta\mu_1' = \mu_1' - [\mu_1']_{\text{inert}}. \qquad (11)$$

As the flame ionization detector did not respond to the inert gas, the first-absolute moments of the inert gas $[\mu_1']_{\text{inert}}$ were calculated from Eq. (8) according to which

$$[\mu_1']_{\text{inert}} = \left[1 + \frac{1-\alpha}{\alpha}\beta\right] z/v_i, \qquad (12)$$

when

$$K_A = 0 \quad \text{and} \quad t_{0A} = 0.$$

It can be seen from Eq. (10) that a plot of

$$\frac{[\Delta\mu_1' - (t_{0A}/2)]}{[(1-\alpha)/\alpha]\beta} \quad \text{vs} \quad z/v_i$$

should yield a straight line passing through the origin. Such plots are shown in Fig. 7 for moments of chromatographic curves obtained at different temperatures for isobutene. The first absolute moments obtained for *n*-butene were found to be the same as for the inert gas [that is $\Delta\mu_1' = 0$] at the temperatures 605.5, 621, and 636.5°K which indicated that the adsorption equilibrium constants were zero. However, plots

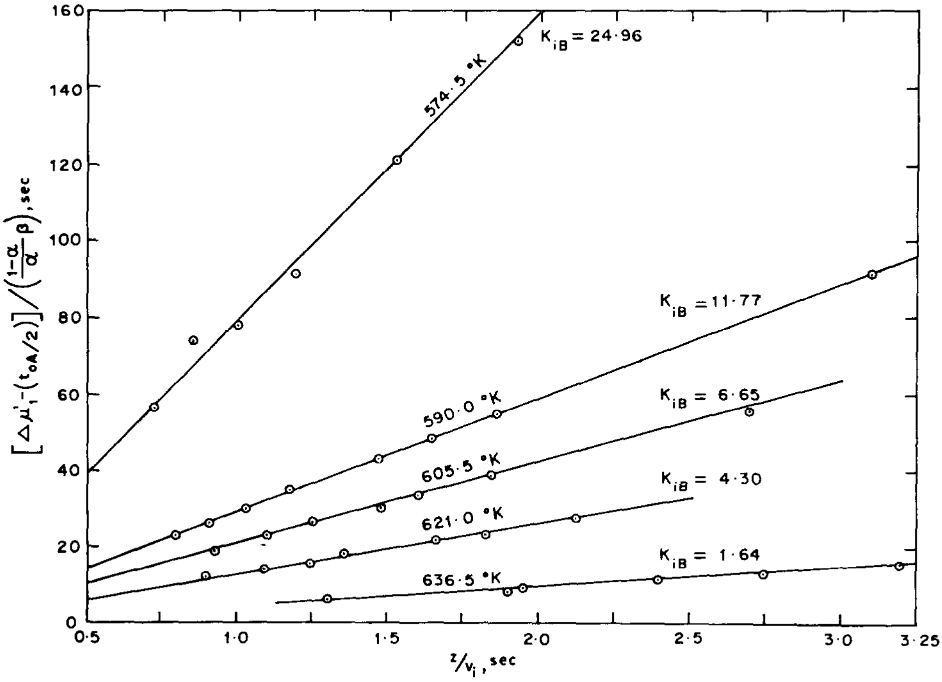

FIG. 7. Chromatography of isobutene on η-alumina (dependence of the reduced first absolute moment on z/v_i).

of

$$\frac{[\Delta\mu_1' - (t_{0A}/2)]}{[(1-\alpha)/\alpha]\beta} \quad \text{vs} \quad z/v_i$$

as shown in Fig. 8 have been drawn for n-butene for three lower temperatures—at which the equilibrium constant showed finite positive values.

RESULTS AND DISCUSSION

The adsorption equilibrium constants for isobutene obtained both from the proposed Hougen–Watson model and by moment analysis of the chromatographic curves are given in Table 2.

One of the strong contending models,

$$r = \frac{k[p_{nB} - p_{iB}/K]}{1 + K_{nB}p_{nB}}, \qquad (13)$$

representing the desorption of isobutene as the controlling step was eliminated during the final selection of a suitable model as the adsorption equilibrium constant for n-butene obtained using the above model was found to be not different from zero at all the temperatures studied. The adsorption equilibrium constant values for n-butene, obtained from the moment analysis of the chromatographic curves were also found to be zero at the temperatures where a comparison between the two methods was attempted. This provides further evidence for rejecting this model in which the adsorption equilibrium constant for n-butene appears as a parameter.

It may be that, with $K_{nB} \approx 0$, one might also theoretically consider the simple power model which contains only the numerator term of Eq. (13). But, as already mentioned, this model was found unacceptable.

It can be seen from Table 2 that the values of K_{iB} and K_{nB} obtained by the two different methods agree to within about 12% [average]. Also an increase in the

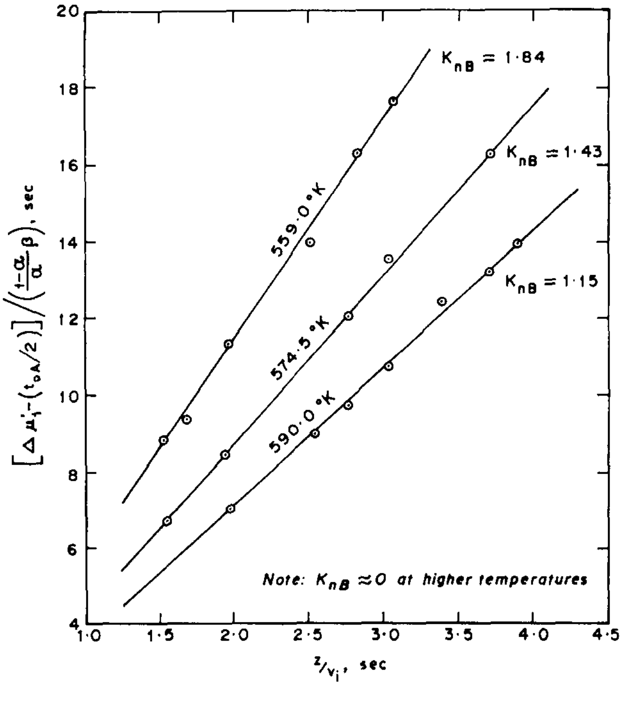

FIG. 8. Chromatography of n-butene on η-alumina (dependence of the reduced first absolute moment on z/v_i).

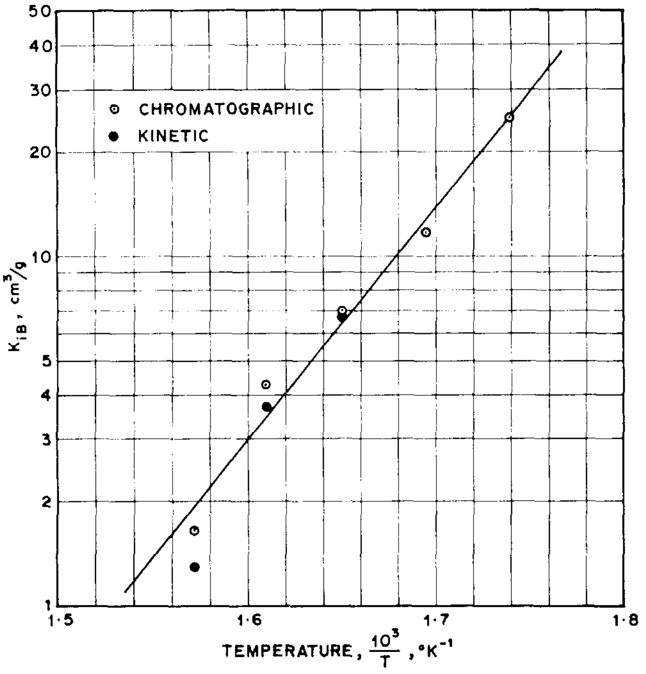

FIG. 9. Van't Hoff plot of the adsorption equilibrium constant.

value of the adsorption equilibrium constant for isobutene with decreasing temperature is clearly discernible. These observations suggest further support to the Hougen–Watson model proposed for the reaction *n*-butene $\rightleftharpoons$ isobutene with η-alumina [containing 2 wt% F] as catalyst.

The difference in the values of the adsorption equilibrium constant for isobutene obtained by the two methods is about 1% at 605.5°K, 14.3% at 621°K, and 20% at 636.5°K.

A Van't Hoff plot based on the chromatographic values is shown in Fig. 9. It can be seen that the kinetic values also fall on the same line, except at the highest temperature where the values calculated by both the methods appear to be slightly lower.

CONCLUSIONS

In this study the validity of statistical methods of kinetic modeling has been examined by determining the parameter values independently from chromatographic studies under reaction conditions. A comparison of the parameter values of the "best" kinetic model with the values obtained from adsorption studies reveals the following:

1. The adsorption constants for isobutene determined by the two methods show agreement to within about 12% over the temperature range studied.
2. The adsorption constants for *n*-butene are zero by both the methods in the temperature range 605.5 to 636.5°K, thus justifying the elimination of the class of models involving K_{nB} in the kinetic analysis.
3. The heat of adsorption for isobutene obtained from the plot of K_{iB} [chromatography] vs $1/T$ is 30.3 kcal/g mole. The values obtained from kinetic data also lie on the same line.

The observations suggest that a combination of kinetic and adsorption studies (the latter at reaction conditions) using practically the same experimental assembly (built around a gas chromatograph) can lead to the selection of an acceptable model. Further work is needed on other systems to confirm this conclusion, with the ultimate objective of establishing the validity of models obtained exclusively from kinetic modeling.

REFERENCES

1. Langmuir, I., *Trans. Faraday Soc.* **17**, 621 (1922).

2. Hinshelwood, C. N., "The Kinetics of Chemical Change." Oxford Univ. Press, New York, 1940.

3. Hougen, O. A., and Watson, K. M., *Ind. Eng. Chem.* **35**, 529 (1943).

4. Yang, K. H., and Hougen, O. A., *Chem. Eng. Progr.* **46**, 146 (1950).

5. Bard, Y., and Lapidus, L., *Catal. Rev.* **2**, 67 (1968).

6. Kittrell, J. R., *Advan. Chem. Eng.* **8**, 98 (1970).

7. Reilly, P. M., and Blau, G. E., *Canad. J. Chem. Eng.* **52**, 289 (1974).

8. Mezaki, R., *AIChE J.* **14**, 984 (1968).

9. Kabel, R. L., and Johanson, L. N., *AIChE J.* **8**, 621 (1962).

10. Schneider, P., and Smith, J. M., *AIChE J.* **14**, 762 (1968).

11. Weisz, P. B., and Prater, C. D., *in* Advances in Catalysis (W. G. Frankenburg, V. I., Komarewsky and E. K. Rideal, Eds.), Vol. 6, p. 143. Academic Press, New York, 1954.

12. Ford, F. E., and Perlmetter, D. D., *AIChE J.* **9**, 371 (1963).

13. Garner, F. H., and Suckling, R. D., *AIChE J.* **4**, 114 (1958).

14. Wilke, C. R., and Hougen, G. A., *Trans. Amer. Inst. Chem. Eng.* **41**, 445 (1945).

15. Choudhary, V. R., and Doraiswamy, L. K., *Ind. Eng. Chem. Process Des. Develop.* **14**, 227 (1975).

16. Choudhary, V. R., *Chem. Ind. Develop.* **8** (7), 32 (1974).

17. Tamaru, K., Catalysts Meeting, Tokyo, Apr. (1957).

18. Tamaru, K., *Bull. Chem. Soc. Japan* **31**, 666 (1958).

19. Tamaru, K., *Nature (London)* **183**, 319 (1959).

20. Nakanishi, J., and Tamaru, K., *Trans. Faraday Soc.* **59**, 1470 (1963).

21. Eberly, P. E., Jr., *J. Phys. Chem.* **65**, 68 (1961).

22. Eberly, P. E., Jr., *J. Phys. Chem.* **65**, 1261 (1961).

23. Kubin, M., *Collect. Czech. Chem. Commun.* **30**, 1104 (1965).

24. Kubin, M., *Collect. Czech. Chem. Commun.* **30**, 2900 (1965).

25. Kucera, E., *J. Chromatogr.* **19**, 237 (1965).